[10]J. A. Krommes, private communication.
[11]K. Molvig, J. E. Rice, and M. S. Tekula, Phys. Rev. Lett. 41, 1240 (1978).
[12]H. P. Eubank, Bull. Am. Phys. Soc. 23, 745 (1978).
[13]M. Murakami, in *Proceedings of the Seventh International Conference on Plasma Physics and Controlled Nuclear Fusion Research, Innsbruck, Austria, 1978* (International Atomic Energy Agency, Vienna, Austria, 1979), paper No. IAEA-CN-37-N-4.
[14]D. L. Jassby, D. R. Cohn, and R. R. Parker, Nucl. Fusion 16, 1045 (1976).
[15]T. Ohkawa, General Atomic Report No. GA-A1-4433, May 1977 (unpublished).
[16]M. Gaudreau *et al.*, Phys. Rev. Lett. 39, 1266 (1977).
[17]A. Gondhalekar, D. Overskei, R. Parker, and J. West, Massachusetts Institute of Technology Plasma Fusion Center Report No. PFC/RR-78-15, 1978 (to be published).

Parametric Instabilities in Lower-Hybrid-Frequency Heating of a Tokamak

T. Imai, T. Nagashima, T. Yamamoto, K. Uehara, S. Konoshima, H. Takeuchi, H. Yoshida, and N. Fujisawa
Japan Atomic Energy Research Institute, Tokai, Naka-gun, Ibaraki-ken, Japan
(Received 25 September 1978; revised manuscript received 9 April 1979)

Decay spectra during the rf heating were identified as the parametric decay into the cold lower-hybrid waves and the ion-cyclotron waves at the plasma surface. The decay instabilities absorbed some fraction of the rf power, hence they affected the plasma heating. However, they did not prevent the penetration of the lower hybrid wave to the plasma center. Drastic reduction of the decay spectra was obtained when the resonant parametric decay condition was destroyed.

Lower-hybrid heating is one of the most attractive techniques for the further heating of a tokamak plasma aiming at a thermonuclear fusion reactor, because of its engineering feasibility.[1] But physical understanding about the interaction of intense rf fields with a tokamak plasma does not seem to be sufficient. Since the required rf power is more than Ohmic heating power for the further heating, nonlinear phenomena will inevitably take place. Among them, parametric instability is the most important in the lower-hybrid range of frequency.[2] In fact, decay spectra were observed in the lower-hybrid heating of the ATC, Wega, and other tokamaks.[3-5] Prokolab has predicted that the heating in the ATC correlated with the presence of the decay spectra.[2,4] In the Wega, correlation between generation of high-energy ions and parametric decay was stressed.[5,6] It is recently discussed the existence of parametric instabilities must lead to blocking and subsequent accumulation of lower-hybrid waves on the low-density surface plasma. The role of parametric instabilities in the lower-hybrid heating experiments is still not clear, despite the enormous works on parametric instabilities.[2,4,6-10]

Lower-hybrid-heating experiments have been successfully carried out in the JFT-2 tokamak at Japan Atomic Energy Research Institute (JAERI), and efficient ion heating was obtained.[11] Parametric decay was also observed in the JFT-2. In this paper, properties of the decay spectra measured with electrostatic probes placed in the plasma periphery will be studied. Identification of the observed decay spectra in plasma heating will be presented.

A 200-kW, 650-MHz (or 750-MHz) radio-frequency system was used for lower-hybrid-heating experiments on the JFT-2. A lower-hybrid-wave launcher was a phased array of four waveguides.[1,12] The dimensions of the each waveguide at a plasma edge were 14 mm $\times$ 290 mm. Experimental parameters are summarized in Table I. Schematic arrangement of the launcher is shown in Fig. 1. The front edge of the launcher was embedded in the scrape-off layer. The electron temperature and density in the scrape-off layer measured with a double probe were $T_e = 15-25$ eV and $n_s = (5-10)\times 10^{17}$ m^{-3}, respectively.

The wave signal was measured with a molybdenum coaxially shielded electrostatic probe, 3 mm long and 1 mm in diameter, immersed in the scrape-off layer. Typical frequency spectra during the rf pulse are shown in Fig. 2(a). Input frequency was 650 MHz. The low-frequency and sideband modes satisfy usual frequency conservation law and the upper sideband intensity is negligibly small. The frequency separation between the pump wave and the nth peak of lower sideband

TABLE I. Parameters of lower-hybrid heating in the JFT-2 tokamak at JAERI.

JFT-2 machine parameters	
Major radius	90 cm
Minor radius	25 cm
Minor wall radius	29 cm
Toroidal magnetic field	9–18 kG
Plasma parameters	
Plasma	Hydrogen plasma
Plasma current	70–160 kA
Ohmic heating power	160–200 kW
Peak electron density	$(1-4.5)\times10^{13}$ cm^{-3}
Peak electron temperature	600–1000 eV
rf heating system	
rf frequency	650 and 750 MHz
Maximum rf power	200 kW
rf pulse duration	1–100 msec
Coupling system	Phases array of four wave guides

mode $(f_0 - f_{-n})$ is plotted in Fig. 3(a). In the figure, solid lines indicate the values of the nf_{ci} ($n = 1, 2, 3, 4$) estimated from the toroidal magnetic field B_t at the plasma center and broken lines are those from the B_t in front of the launcher. It is seen that the experimental points fit the broken lines well. $0 < [(f_0 - f_{-n}) - nf_{ci}]/f_{ci} < 0.2$ is satisfied, if the B_t in front of the launcher is used. Dispersion relation of the nth-harmonic ion-cyclotron wave is approximately given by

$$\omega \simeq n\omega_{ci} + n\omega_{ci} I_n(b_i) e^{-b_i} T_e/T_i, \quad (1)$$

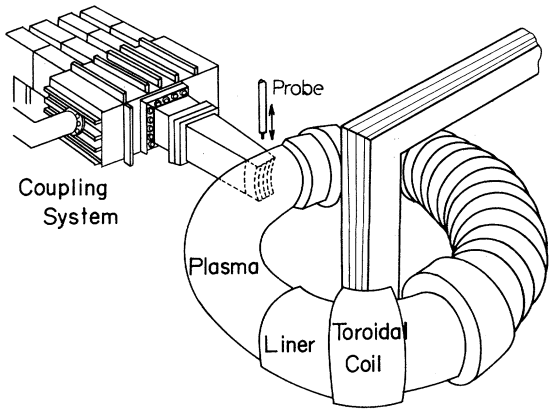

FIG. 1. Schematics of a waveguide coupling system on the JFT-2 tokamak.

where $b_i = (k_\perp V_{Ti}/\omega_{ci})^2/2$ and the I_n is nth modified Bessel function. The frequency shift from nf_{ci} is explained very well by Eq. (1) with the parameters $k_\perp = k_D/4$, $T_e = T_i$, and $k_D^2 = n_e e^2/\epsilon_0 T_e$, so that the low-frequency decay waves may be identified as the electrostatic ion-cyclotron waves excited in front of the launcher.

Dependence of the decay wave amplitude on rf power is shown in Fig. 3(b). The threshold power of the onset of parametric instabilities is $P_{\text{thresh}} = 3-5$ kW. It should be noted here that the amplitude has a tendency to be saturated at a power of 40 kW. Since the e-folding length of the density gradient at the plasma surface (5–10 cm) is much larger than the pump width of radial direction (~ 1 cm), the threshold is determined from the finite-extent pump effect as follows[10]:

$$U/C_s \simeq 100(M/m)^{1/2}(\lambda_D/L_{0z})Q^{1/2}, \quad (2)$$

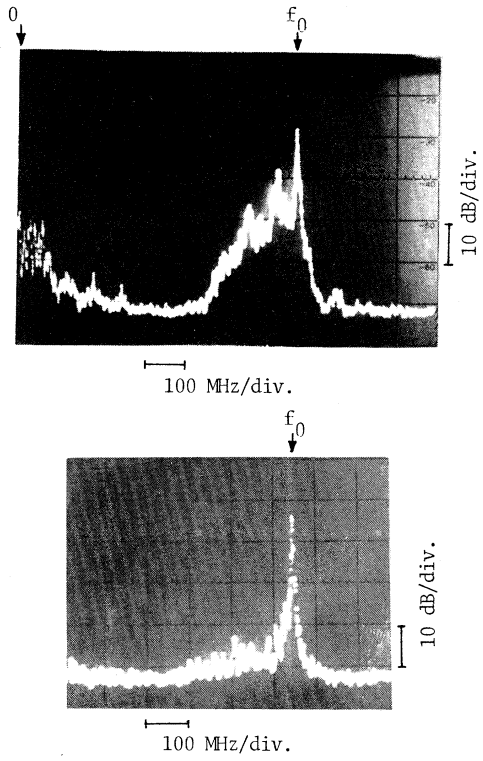

FIG. 2. Parametric decay spectra during the rf pulse. (a) Spectrum in the frequency range from 0 to 1 GHz, where $P_{rf} = 60$ kW, pump frequency $f_0 = 650$ MHz, phase difference between adjacent waveguides $\Delta\varphi = 90°$, mean plasma density $\bar{n}_e = 0.9\times10^{19}$ m^{-3}, and $B_t = 1.3$ T. (b) Spectrum around the pump frequency $f_0 = 750$ MHz. $\bar{n}_e = 2.7\times10^{19}$ m^{-3}, and $P_{rf} \simeq 150$ kW.

where

$$Q=(\pi)^{1/2}[\omega_1/k_{\parallel}V_{Te}]\{1+(T_e/T_i)^{3/2}(M/m)^{1/2}I_1(b_i)\exp(-b_i)\exp[-(\omega-\omega_{ci})^2/(k_{\parallel}V_{Ti})^2]\},$$

$C_s^2=eT_e/M$, $\lambda_D=1/k_D$, L_{0z} is the width of a launcher, M the ion mass, m the electron mass, and $U=E_r/B_t$. From our conditions $\omega_0 \gg \omega_{pi}$, so that E_r is expressed as

$$E_r^2=(\omega_{pe}/\omega_0)(2p\eta_0\lambda_0/L_{0z}^2L_{0y})P_0, \quad (3)$$

where P_0 is the input rf power, $p=L_{0z}/\lambda_{0z}$ with λ_{0z} being the parallel wavelength, η_0 the intrinsic impedance ($\sim 380\ \Omega$), λ_0 the vacuum wavelength, and L_{0y} the height of the launcher.[7] With use of the parameters $n_s=5\times10^{17}$ m^{-3} and $T_e=20$ eV in the scrape-off layer, Eqs. (2) and (3) give $P_{\text{thresh}}\simeq 5$ kW which explains the observed threshold power. Threshold power depends on the density as $P_{\text{thresh}} \propto n_e^{-3/2}$ from Eqs. (2) and (3). This is shown most clearly in Fig. 4.

One of the remarkable properties of the decay spectra is frequency spread of the instabilities. Dependence of the frequency spread Δf (10 dB higher than the noise level) on $(f_{pi}^{(s)}/f_0)^2 \propto n_i$ is shown in Fig. 5, where $f_{pi}^{(s)}$ is the ion plasma frequency at the plasma surface. The spread increases with an increase in density. But under the condition $f_0/f_{pi}^{(s)} \lesssim 2$, drastic reduction of the decay instabilities was obtained [Fig. 2(b)]. This reduction is clearly explained by the theoretical prediction that the resonant parametric decay into the cold lower-hybrid waves and the ion-cyclotron waves does not occur when the condition $f_0/f_{LH}>2$ is destroyed, since $f_{LH}\simeq f_{pi}^{(s)}$, where f_{LH} is the local lower-hybrid frequency.[10]

In our heating experiments, an increase in ion temperature, decay spectra, and high-energy ion tail were observed when a turning point was near the center.[11] Without the turning point in the plasma, bulk ion heating did not occur and similar decay spectra with high-energy ion tail were observed. The gross efficiency of the ion heating ($\bar{n}\Delta T_i$) is also plotted in Fig. 5 (closed circles) as a function of the density at the plasma surface. The maximum ion heating took place at $f_{pi}^{(s)}/f_0 \simeq 0.5$ when the remarkable reduction of the parametric decay was obtained. This density corresponds to $f_{LH}^{(0)}/f_0\simeq 1.2$, where $f_{LH}^{(0)}$ is the lower-hybrid frequency at the plasma center. No ion heating was observed when the turning point was

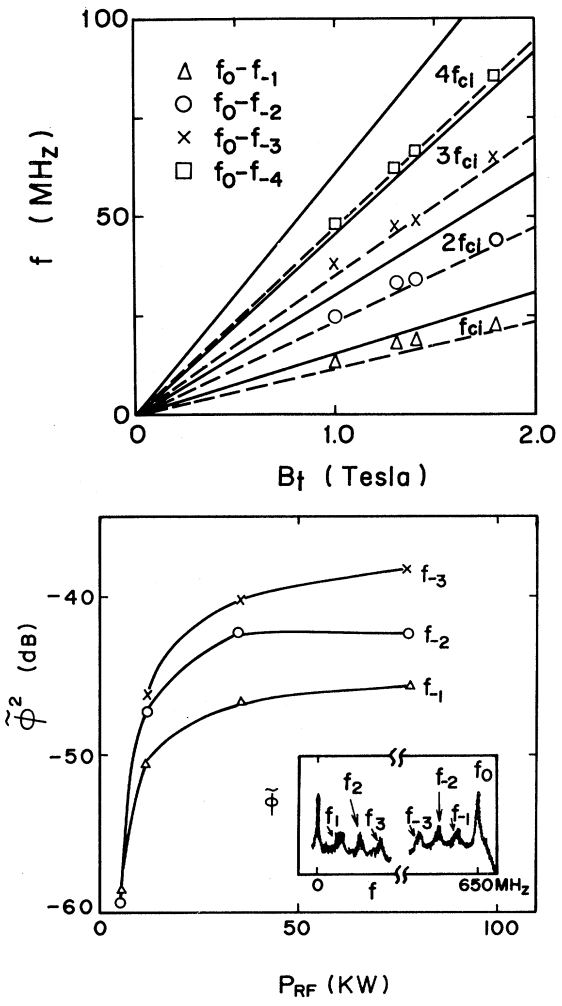

FIG. 3. (a) Frequencies of peaks of lower sideband modes vs toroidal magnetic field at at the center; solid lines indicate nf_{ci} at the plasma center and broken lines are those in front of the launcher. (b) Lower sideband amplitude vs P_{rf}.

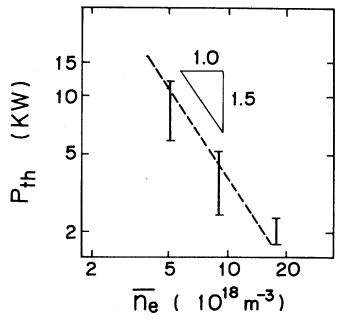

FIG. 4. Threshold power of parametric instabilities vs mean plasma density. Broken line is calculated from the theory.

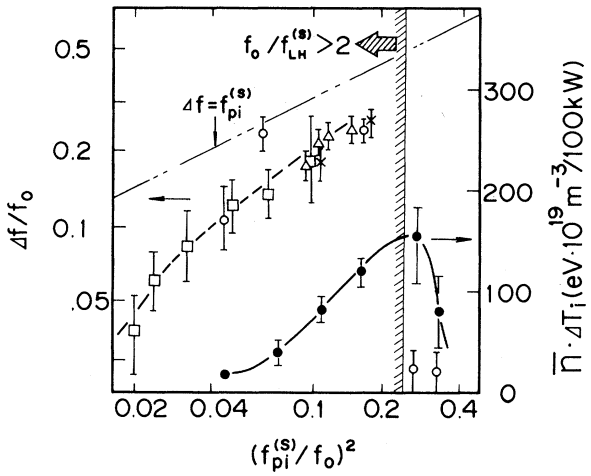

FIG. 5. Frequency spread Δf and gross ion heating efficiency $\bar{n}\Delta T_i$ as a function of $(f_{pi}^{(s)}/f_0)^2$. Toroidal fields of the points are as follows: open circles, $B_t = 1.8$ T; open squares, $B_t = 1.4$ T; triangles and crosses, 1.3 T, and closed circles, $B_t = 1.8$ T. The dotted line indicates that of $\Delta f = f_{pi}^{(s)}$.

not in the plasma (very low density) or was far from the plasma center (very high density). If we assume that ions absorb the wave energy at the turning point, maximum ion heating occur at $f_{pi}^{(s)}/f_0 = 0.3-0.4$ when the turning point is near the plasma center. This discrepancy indicates some fraction of the rf power was absorbed by the parametric instabilities at the plasma surface. However the problem of the surface absorption does not seem to be fatal, since the decay wave amplitude tends to be saturated with increasing the transmitted power, and the increment of the bulk ion temperature is nearly proportional to the input rf power at a higher power level than ~ 40 kW as reported previously.[11] In addition, the change in the heating efficiency in both regions $f_{pi}^{(s)}/f_0 \gtrless 0.5$ is not abrupt. It is important to notice that few decay waves were observed beyond the critical density and still ion heating was observed. Physical details of the ion heating will be described in a separate publication.

In summary, the parametric decay into the cold lower-hybrid waves and the ion-cyclotron waves was observed. The observed decay was excited at the plasma surface, hence some fraction of the rf energy was absorbed at the plasma surface. The parametric instabilities do not appear to prevent the penetration of the launched lower-hybrid wave to the plasma center. The reduction of parametric instabilities as well as the maximum ion heating were obtained under the condition $f_0/f_{pi}^{(s)} \lesssim 2$. More efficient ion heating will be expected if parametric instabilities at the plasma surface are well controlled.

We wish to thank all the other members of the JFT-2 for their discussions. We also wish to thank Dr. Y. Tanaka, Dr. H. Shirakata, Dr. Y. Obata, and Dr. S. Mori for their encouragements of this work.

[1]M. Brambilla, P. Lallia, and K. Nguyen Trong, Association EURATOM–Commissariat à l'Energie Atomique Report No. EUR-CFA-FC-792, 1975 (unpublished); M. Brambilla, Nucl. Fusion 16, 47 (1976); P. Lallia, in *Proceedings of the Second Topical Conference on rf Plasma Heating, Lubbock, Texas, 1974* (Texas Tech. Univ., Lubbock, Tex., 1974), p. C-3.

[2]M. Porkolab, Nucl. Fusion 18, 367 (1978).

[3]V. V. Alikaev *et al.*, Zh. Tekh. Fiz. 45, 523 (1975) [Sov. Phys. Tech. Phys. 20, 327 (1975)].

[4]M. Porkolab, S. Bernabei, W. M. Hooke, R. W. Motley, and T. Nagashima, Phys. Rev. Lett. 38, 230 (1977).

[5]P. Blanc *et al.*, in *Proceedings of the Third International Meeting on Theoretical and Experimental Aspects of Heating of Toroidal Plasma, Grenoble, France, 1976*, edited by T. Consoli (Commissariat à l'Energie Atomique, Grenoble, France, 1976), Vol 2, p. 251.

[6]S. Takamura and P. Javel, Association EURATOM-Commissariat à l'Energie Atomique Report No. EUR-CFA-FC-863, 1976 (unpublished).

[7]R. L. Berger, Liu Chen, P. K. Kaw, and F. W. Perkins, Phys. Fluids 20, 1864 (1977).

[8]W. M. Hooke and S. Bernabei, Phys. Rev. Lett. 29, 1218 (1972).

[9]K. Yatsui and T. Imai, Phys. Rev. Lett. 35, 1279 (1975).

[10]M. Porkolab, Phys. Fluids 20, 2085 (1977).

[11]T. Nagashima and N. Fujisawa, in *Proceedings of the Joint Varenna-Grenoble International Symposium on Heating in Toroidal Plasma, Grenoble, France, 3–7 July 1978*, edited by T. Consoli and P. Caldirola (Pergamon, Elmsford, N. Y., 1979), Vol. 2, p. 281.

[12]S. Bernabei, *et al.*, Nucl. Fusion 17, 929 (1977).

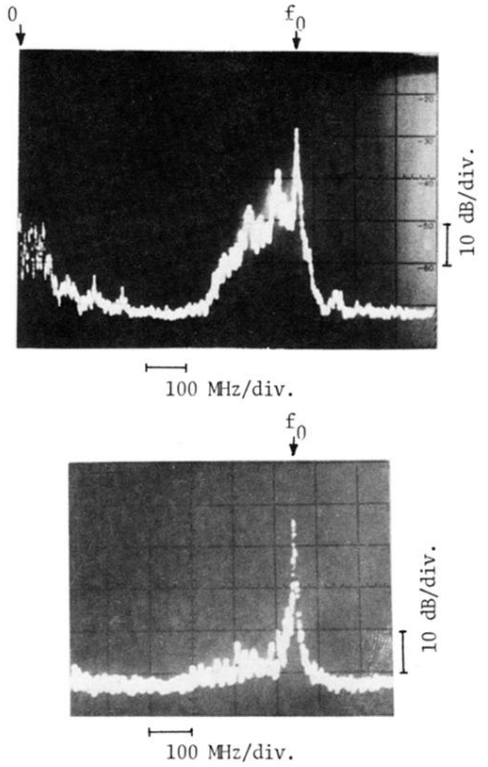

FIG. 2. Parametric decay spectra during the rf pulse. (a) Spectrum in the frequency range from 0 to 1 GHz, where $P_{rf} = 60$ kW, pump frequency $f_0 = 650$ MHz, phase difference between adjacent waveguides $\Delta\varphi = 90°$, mean plasma density $\bar{n}_e = 0.9 \times 10^{19}$ m^{-3}, and $B_t = 1.3$ T. (b) Spectrum around the pump frequency $f_0 = 750$ MHz. $\bar{n}_e = 2.7 \times 10^{19}$ m^{-3}, and $P_{rf} \simeq 150$ kW.